Refereed Proceedings

The 12th International Conference on Fluidization - New Horizons in Fluidization Engineering

Engineering Conferences International *Year* 2007

Solids Flux, Velocity and Local Solid Fraction Measurements in a CFB Riser

Ronald W. Breault* Christopher Guenther†

*National Energy Technology Center, ronald.breault@netl.doe.gov

†National Energy Technology Center

Solids Flux, Velocity and Local Solid Fraction Measurements in a CFB Riser

Ronald W. Breault and Christopher Guenther
National Energy Technology Center
U.S. Department of Energy
3610 Collins Ferry Road, Morgantown, WV 26507-0880

ABSTRACT

In this investigation a fiber-optic probe and an extraction solids probe are used to measure particle velocities and solids flux values. These are subsequently used to determine the local solids fractions as a function of radial position in a cold flow circulating fluidized bed (CFCFB) in operation at the National Energy Technology Laboratory (NETL). Measurements were taken under several separate operating conditions ranging from dilute up-flow to core-annular flow to fast fluidization using nominal 800 micron cork particles. The solids properties and test operating conditions were chosen particularly to provide dynamic similitude between the test data and the operation of a high temperature, high pressure gasifier. The data from these conditions is different in many ways from the data developed using more conventional solids (glass, FCC, and sand) at atmospheric conditions. In this paper, the data from the middle of the riser corresponding to a height of nominally 8 m is presented. Average solids fractions are compared to the apparent values based upon the pressure drop and the near wall measurements are compared to LDV generated solids fraction values, showing good agreement with both. Also, the radial profiles tended to be relatively flat with a sharp rise at the wall.

INTRODUCTION

There is a paucity of local data in moderately dense to dense risers that exhibit a great deal of solids down-flow, operation in the core-annular regime. A number of publications can be found to provide local data in mostly dilute conditions [1, 2, 3, 4, 5, and 6]. Gidaspow and Huilin [1] and Tartan and Gidaspow [2] have published data in dilute conditions having an apparent solids fraction of 0.02. In that work, they use PIV techniques to probe a 0.076 m riser to provide local solids velocities. Then they use the velocities to provide granular (particulate) turbulent kinetic energy values. These experiments were conducted with 520 μm glass beads with a density of 2460kg/m^3.

Brereton and Grace et al [3] conducted tests in a 0.152 m riser, providing local solids fractions with a capacitance probe. This work was also conducted in a dilute regime with the apparent solids fraction of about 0.02.This work showed the existence of a dense annular region near the wall. This annular region had a solids fraction 5 to 10 times greater than the apparent average. The work was conducted with 146 μm sand particles with a density of 2650 kg/m^3.

Nieuwland et al. [4] conducted work in a two inch riser presenting both local solids fractions and local solids velocities for dilute upflow conditions. Integrated solids flux calculations agreed quite well with the measured flux values. The error was all in one direction and attributed to solids downflow at the wall with the greatest error occurring at the lowest gas velocity. The apparent solids fractions were typically in the range of 0.02 to 0.05. This work was conducted with 129 μm sand particles with a density of 2540 kg/m^3.

Yan et al. [5] conducted a set of experiments in a 0.076 m riser, measuring both local solids fraction and local solids velocity, both with optical probes. The work showed the existence of a dense annual region at the wall that was 2 to 4 times the average solids fraction obtained by integration of the local measurements which ranged from 0.05 to 0.15. The integrated solids flux calculations were not reported for comparison with the measured circulation rate. This work was conducted with 67 μm FCC particles with a density of 1500 kg/m^3.

Zhu et al. [6] conducted experiments in a 0.100 m riser to compare the measured solids flux to the calculated solids flux from integrated local measurements of solids velocity and solids volume fraction. The comparison was within 5% for experiments conducted over a wide set of conditions with gas velocities ranging from 3.7 to 10.2 m/s and solids flux values ranging from 49 to 205 kg/m^{2}s. Local solids fraction data was apparently obtained to make the calculation but was not reported. This work was conducted with 67 μm FCC particles with a density of 1500 kg/m^3.

The limited data, particularly for more dense flows, lead to experiments being conducted to generate validation data for the simulation code MFIX. These experiments were conducted in optically dense conditions that had an apparent solids fraction based upon pressure drop data ranging nominally from 2 to 12%. During these experiments, local solids flux measurements were taken with an extraction probe. Care was taken to ensure that the samples were taken in the most isokineticly manner possible. This methodology is reported by Miller[7]. Also, local solids velocity data was taken with an optical probe. These values and the calculated local solids fractions are reported.

EXPERIMENTAL METHODS AND TEST MATRIX

The test unit configuration is shown in Figure 1 and described by Shadle et al [8]. The solids enter the riser from a side port 0.23-m in diameter and 0.27-m above the gas distributor. Solids exit the riser through a 0.20-m port at 90^o about 1.2-m below the top of the riser at a point 15.3-m above the gas distributor. Riser gas velocities were corrected for temperature and pressure as measured at the base of the riser. The air's relative humidity was maintained at 20% to minimize effects of static charge building up on the solids. The riser pressure drop resulting solely from gas flow was found to be negligible over those flow rates studied.

Twenty incremental differential pressures were measured across the length of the riser using transmitters calibrated within 0.1 % of full-scale or about 2 Pa/m. The primary response measurement was the overall riser pressure differential and it was calibrated within 0.45 Pa/m. Mass circulation rate was continuously recorded by measuring the rotational speed of a twisted spiral vane located in the packed region of the standpipe bed [9]. This volumetric flow measurement was converted to a mass flux using the measured packed bed density. Over the range of operating conditions studied the

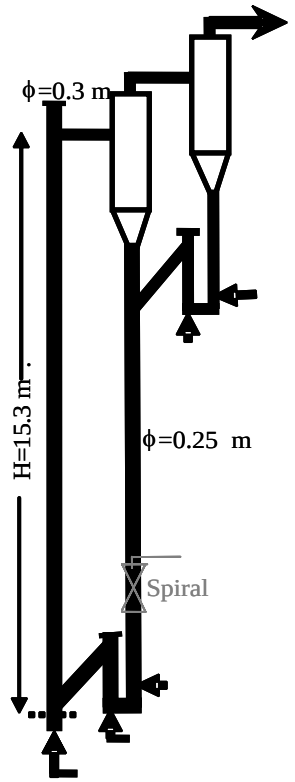

Figure 1. Schematic of cold flow CFB.

packed bed void fraction at the point of measurement was assumed to be constant.

Fluidization bed material properties are presented elsewhere, see Breault [10]. A relatively light bed material of particle size 812 μm determined by the volume to surface area ratio denoted by d_{32} was selected to generate data relevant for advanced high-pressure coal conversion processes. According to a Buckingham-Pi analysis of the riser in a CFB the ratio of gas: solids density is a critical factor, important in scaling from a model, such as these cold flow tests, to a prototype application, such as a high pressure and high temperature transport reactor. Cork offers an excellent bed material which when tested at ambient conditions in air yields a similar density ratio to that of coal processed at 10-20 atmospheres and 1000 C.

The particle density was measured using water displacement taking care to wet the surface completely. The cork surface is sufficiently hydrophobic to avoid filling any porosity with water. The particle size was measured using standard sieve analysis. The size distribution is displayed elsewhere, see Breault [10]. The minimum fluidization velocity was measured in the loopseal by closing the slide gate valve in the standpipe and increasing the gas velocity while measuring an incremental pressure drop across the loopseal. In addition, the shape factor for this natural wood material is expected to be comparable to that of coal that was derived from woody tissues and retains much of its morphology.

A statistically designed composite test matrix was conducted in randomized order by varying the superficial riser gas velocity and the solids circulation rate over five equally spaced levels for each. The riser gas flow was varied between 3.7 and 5.5 m/s while the solids circulation rate was varied between 0.25 and 1.25 kg/s. The test matrix included 9 unique steady state conditions with the center point being duplicated to evaluate response uncertainty. The operator varied operating conditions by adjusting the riser flow or solids circulating rate while maintaining constant system pressure at the base of the riser using feedback control of the back pressure control valve at the exit of the second cyclone. The solids circulation was varied by controlling the aeration at the base of the standpipe and when necessary by adjusting the total system inventory to increase the standpipe bed height. Steady state conditions were defined as holding a constant set of flow conditions and maintaining a constant time averaged response in the pressure differentials and solids circulation rate over a five-minute period.

In Figure 2 the test matrix is overlaid on a flow regime map containing representative voidage profiles where the specific test conditions are shown by the spheres. The relative size of the spheres reflects apparent solids holdup or ΔP_{riser} while maintaining constant system pressure at the base of the riser. The set of 9 conditions, gas flow rate and solids flow rate pairs, define the conditions that were tested extensively. These conditions spanned a range of operating conditions from dilute upflow to core annular flow, and approaching dense upflow.

RESULTS AND DISCUSSION

The axial distribution of the solids for all conditions was essentially uniform except for relatively short (6-9 diameters) entrance and exit effects as determined by the axial pressure profile [8]. In other words, the apparent solids fraction, (1-ε), was not a function of height for each test and ranged between 0.016 and 0.113 for the test matrix. Table 2 gives the values of the loading ratio at each of the test conditions. In the experiments reported herein, only five conditions are discussed. Those experiments are TC1, TC3, TC5, TC7 and TC9. The effect of gas velocity can be seen by comparison of conditions TC3, TC7 and TC9 for a fixed solids flow and the effect of solids flow can be seen by comparison of conditions TC1, TC5 and TC9 for a fixed gas velocity.

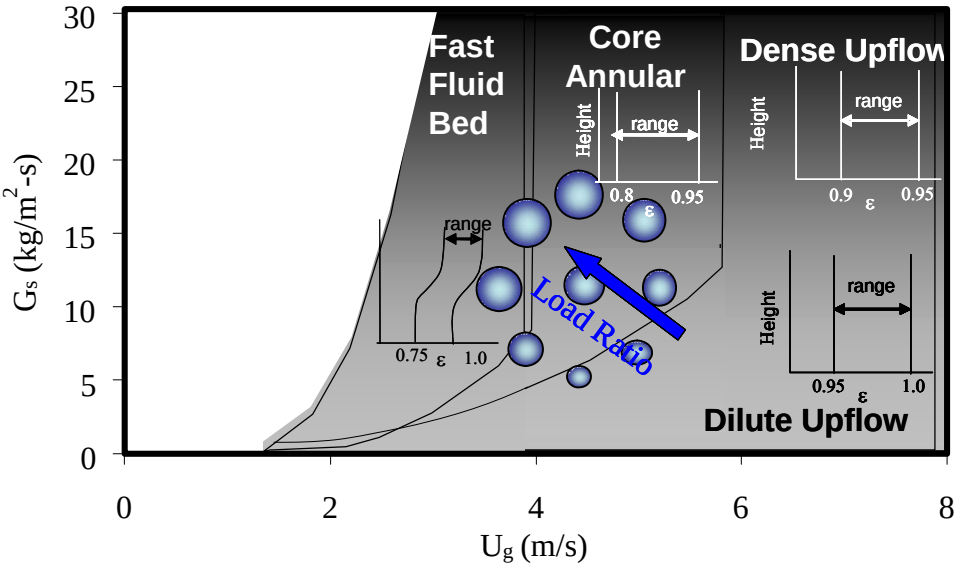

Figure 2. Test matrix with cork in the CFB flow regimes.

Table 1. Loading ratios as a function of the test condition

Test Condition	TC1	TC2	TC3	TC4	TC5	TC6	TC7	TC8	TC9
Ms (kg/hr)	4545	4013	2727	1442	909	1442	2727	4013	2727
Ug (m/s)	4.65	5.24	5.49	5.24	4.65	4.06	3.81	4.06	4.65
Loading Ratio	2.982	2.336	1.516	0.839	0.596	1.084	2.183	3.017	1.789

Solids Flux Measurements.

The integrated local solids flux measurements at the 8.5 m level are presented in Figure 3 as compared to the setpoint values for the spiral, continuous solids flow rate measurement device. The agreement is quite well, providing confidence in the use of the spiral as a control and monitoring device for the cold flow facility.

The solids flux profiles for test conditions TC1, TC3, TC5, TC7 and TC9 are presented in Figure 4. For simplicity in making comparisons between the charts, the "y" axis for each of these graphs is labeled only on the TC7 chart and the "x" axis label appears only on the TC5 chart. The vertical three charts are at a constant gas velocity of 4.65 m/s and the three horizontal charts are for a constant solids flow rate of 2727 kg/hr. Also, the downward flux values are represented by squares and the upward flux values by diamonds.

Looking at TC5, TC9 and TC1 in that order, it can be seen that for a low solids flow rate of 909 kg/hr (TC5), there is very little down flow of solids. In the center three equal area positions, no downward solids flux values could be obtained. Only at the outer two equal area locations were down flowing solids detected and these values were essentially zero. The upward solids flux profile was essentially independent of radial position and equal to 0.63 kg/m^{2}s. Moving from the TC5 chart to the TC9 chart to the TC1 chart, two observations can easily be seen. The first of these is that the number of radial positions where downward flowing solids could be detected increases from 2 to 4 to all 5 locations in the heaviest loaded condition. The second observation is that the difference between the maximum solids flux values at the

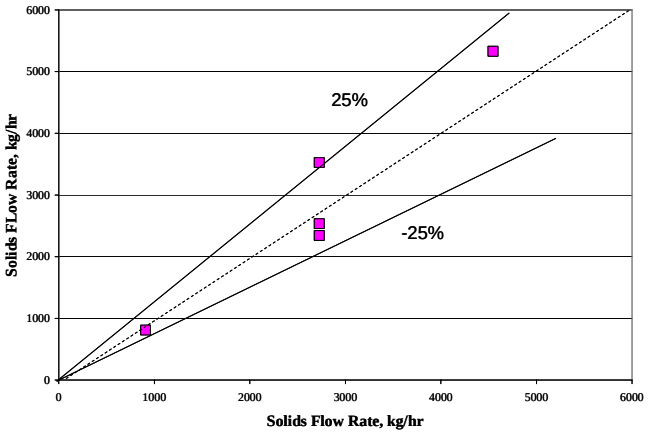

center and the minimum values at the wall increases from the most dilute case (TC5) to the densest case (TC1). This difference increases from about 4 to about 6 kg/m^{2}s for the downward flowing solids and from about 5 to about 10 kg/m^{2}s for the upward flowing solids.

Figure 3. Comparison of spiral flow rate to integrated flux rate.
Figure 4. Solids flux profiles

Essentially, the same trends can be see in Figure 4 when the charts TC3, TC9 and TC7 are reviewed from right to left, moving from the most dilute case for a solids flux rate of 2727 kg/m2s and a gas velocity of 5.49 m/s to the most dense case with a gas velocity of 3.81 m/s.

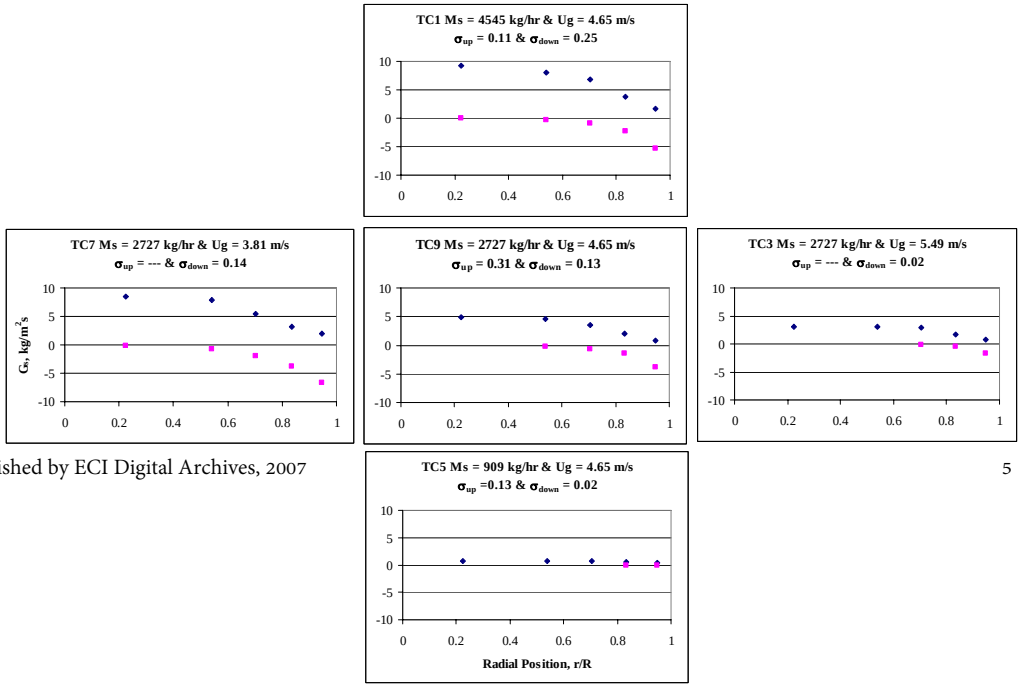

Solids Velocity Measurements.

A fiber optic probe was used to measure solid particle velocity profiles in the cold flow circulating fluidized bed (CFCFB) riser at the same conditions and locations that the solids flux measurements were take. The details of the probe and methodology development were reported by Zinn [11]. The local solids velocity data are presented in Figure 5. Figure 5 is configured identically to Figure 4. That is, the "y" axis is labeled in the TC7 chart and the "x" axis is labeled in the TC5 chart. Also, the squares are for down flowing solids and the diamonds are for up flowing solids. The solids velocity data in Figure 5 show the same trends as the solids flux data in Figure 4. Looking first at the TC5 chart and moving vertically to TC9 and then to TC1, it can be seen that the downward velocity gets more negative and the upward velocity gets more positive. Also, the highest velocities are in the center and the lowest at the wall. The standard deviations for the data are not reported in the Figure 5 as in Figure 4 due to the non-Gaussian distributions of the velocity distributions. The average skewness for the up flowing solids is 8.2 and for the down flowing solids is 1.0.

An interesting observation in the data for solids down flow is that there appears to be a maximum downward velocity around -1 m/s. This is seen by comparison of TC9 to TC1 and TC7. The downward velocity does not increase, but the region of influence does. In other words, solids are moving downward at the maximum downward velocity for TC7 through 60% of the riser cross section.

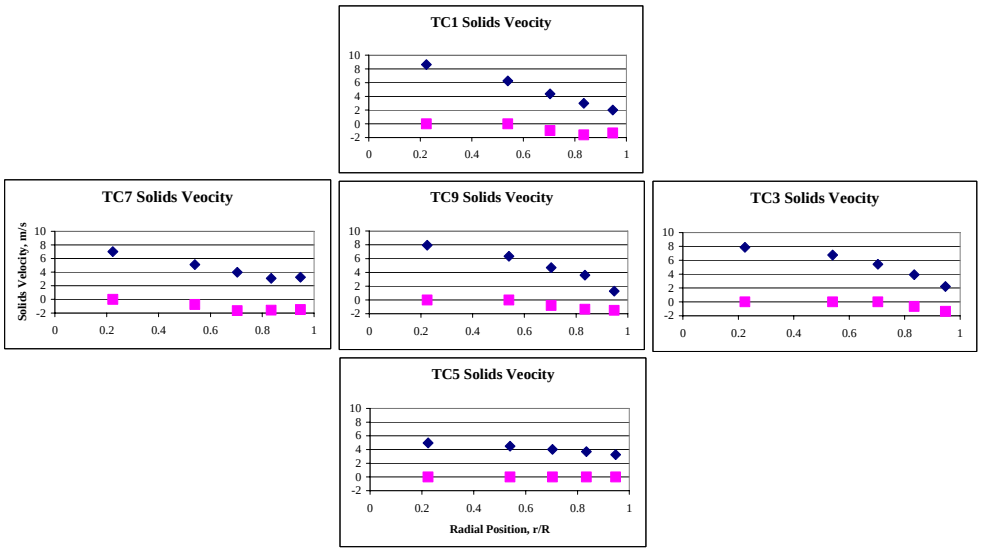

Figure 5. Solids velocity data.

Calculated Solids Faction Values.

The local solids fraction values are calculated from the continuity relationship, $(1-\varepsilon) = G_s/\rho_s U_s$, where $(1-\varepsilon)$ is the solids fraction, G_s is the solids flux (presented in Figure 4), U_s is the solids velocity (presented in Figure 5) and ρ_s is the solids density. The solids fraction is calculated for the solids flowing upward and for the solids flowing downward. These two values are then time weight averaged from the fiber optic velocity probe data with the results presented in Figure 6. The error bars on the data in Figure 6 are obtained by propagating the standard deviation data presented in Figure 4 for the solids flux values. The "error" associated with the width and skewness of the solids velocity data were not incorporated into this propagation. The larges

error is 17% of the solids fraction value and that occurs in TC5 where the solids flux values are small compared to the other test conditions.

The general trends are consistent with expectations, that is for conditions TC5, TC9 and TC1 the solids fraction increases with increasing solids flow rate. Also, for conditions TC3, TC9 and TC7 the solids fraction increases with decreasing gas velocity. In addition, the value of the solids fraction at the wall, with the exception of the most dilute condition (TC5), is the greatest. The annular region thickness can be estimated from the profiles presented in Figure 6. For conditions TC1, TC3, TC7, and TC9, the thickness appears to be independent of the operating conditions and comprises about 20% of the riser radius.

As a check for the magnitude of the solids fraction values calculated, the values near the wall are compared to values obtained with the LDV, Figure 7[12]. The LDV values are obtained for conditions in which clustering was observed as defined by Breault [10]. In general, there is very good agreement between the LDV measured solids fractions and the calculated values based upon the solids flux and solids velocity values. The greatest difference between the two values is in the most dilute condition (TC5). It is quite possible that the solids value at the wall is much greater than the value just 0.5 cm from the wall. Yan et al. [5] reports similar observations. A second check on the data is a comparison of the local solids fraction values to the apparent solids fraction values as presented in Figure 8.

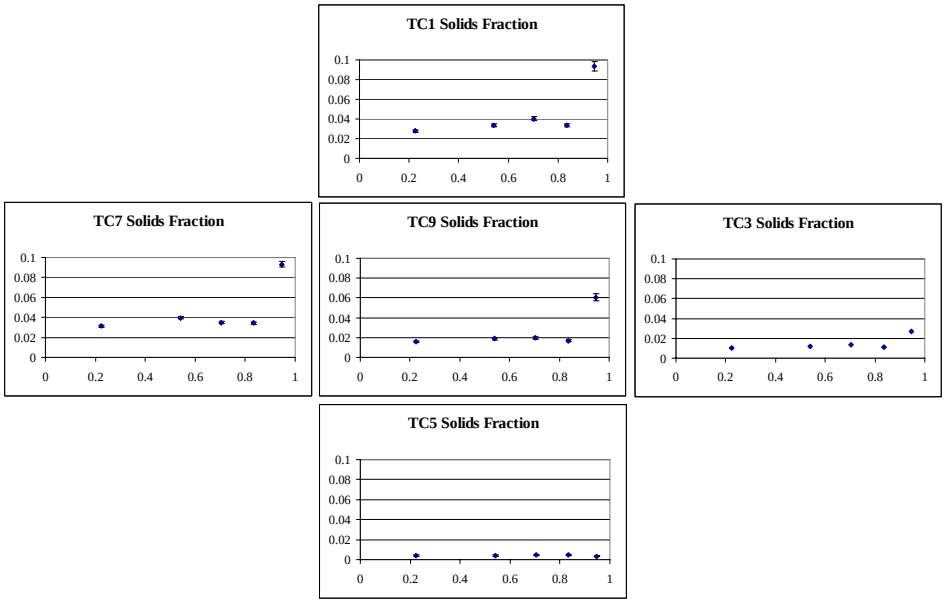

Figure 6. Calculated solids fraction values

CONCLUSIONS

Solids flux and velocity measurements were made and presented. These values were used to calculate the solids fraction. The integrated solids fractions profiles are similar to the apparent solids fractions. Also, the values near the wall approach are similar to the wall measurements obtained from LDV data. Collectively, these two observations provide confidence in the calculated local solids fraction values. Another interesting trait that is seen in the data is that the annular region thickness is independent of the gas and solids values, being about 20 percent of the riser radius. This observation is also seen in Yan's work [5].

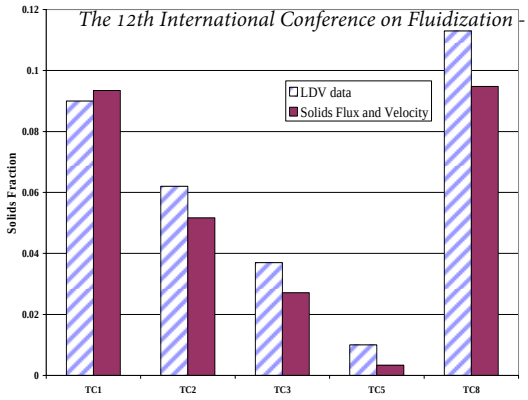

Figure 7. Comparison of solids fractions near and at the wall

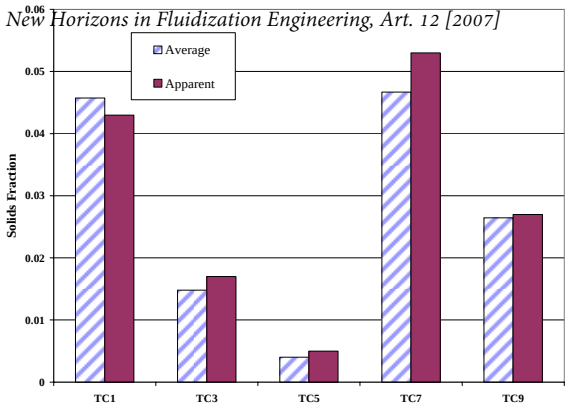

Figure 8 Comparison of apparent and average local solid fractions

REFERENCES

1. Gidaspow, D., Huilin L. "Equations of state and radial distribution functions of FCC particles in a CFB", *AIChE Journal;*1998;44(2), 279-293.Lu Huilin
2. Tartan, M. and Gidaspow, D. "Measurement of granular temperature and stresses in risers", *AIChE Journal,* 2004;50(8), 1760-1775.
3. Brereton, C.M.H. and Grace, J.R., "Microstructural aspects of the behavior of circulating fluidized beds", Chemical Engineering Science, Vol 48, No. 14, pp. 2565-2572, 1993.
4. Nieuwland, J.J., Meijer, R., Kuipers, J. A. M., van Swaaij, W. P. M., "Measurements of Solids Concentration and Axial Solids Velocity in Gas-solid Two-phase flows", *Powder Technology*, 87, pp. 127-139, (1996).
5. Yan, A.,, Parssinen, J.H., and Zhu, J.-X., "Flow properties in the entrance and exit regions of a high-flux circulating fluidized bed riser", Powder Technology, 131 (2003) 256-263.
6. Zhu, J.-X., Li, G.-Z., Qin, S.-Z., Li, F.-Y., Zhang, H., Yang, Y.-L., "Direct measurements of particle velocities in gas-solids suspension flow using a novel five-fiber optical probe", Powder technology, 115 (2001) 184-192.
7. Miller, A.L. "Extraction Probe Analysis of Cork Particles in the Riser of a Circulating Fluidized Bed", DOE Final Report. DE-AP26-01NT00768 (2002).
8. Shadle L.J., Monazam, E.R., Mei, J.S., "Characterization of Operating Flow Regimes In a Cold Flow", J. R. Grace, J. Zhu, H. de Lasa (Ed.), *Circulating Fluidized Bed Technology VII*, Ottawa, Canada, 2002; 255-262.
9. Ludlow, J.C., Shadle, L.J., Syamlal M. "Method to continuously monitor Solids Circulation Rate", J. R. Grace, J. Zhu, H. de Lasa (Ed.), *Circulating Fluidized Bed Technology VII*, Ottawa, Canada, 2002; 513-520.
10. Breault, R.W., Ludlow, J.C., Yue, P.C., "Cluster Particle Number and Granular Temperature of Cork Particles at the Wall in the Riser of a CFB", Powder Technology, 2005;149, 68-77.
11. Zinn, A., Monazam, E., Spenik, J. and Ludlow, J.C., "REM Laser Probe Contract Results and Summary", OSTI Report No. DOE/NETL-2006/1229.
12. Breault, R. W., Pandy, P. and Shadle, L. J., "Granular Temperature and Turbulent Kinetic Energy of Cork Particles in the Riser of a CFB", CFB8, Hangzhou, China.